Two bonding configurations for individually adsorbed C_{60} molecules on Au(111)

Lin Tang,[1] Xin Zhang,[1] Quanmin Guo,[1] Yu-Ning Wu,[2] Lin-Lin Wang,[2] and Hai-Ping Cheng[2]
[1]*School of Physics and Astronomy, University of Birmingham, Edgbaston, Birmingham B15 2TT, United Kingdom*
[2]*Department of Physics and the Quantum Theory Project, University of Florida, Gainesville, Florida 32611, USA*
(Received 7 July 2010; published 9 September 2010)

Two distinct bonding configurations have been identified for individually adsorbed C_{60} molecules on the elbow site of Au(111) using scanning tunneling microscopy: a strong bonding configuration where the molecule sits in a single-atomic-layer-deep pit and a weak bonding configuration where the molecule sits directly above the dislocation of the elbow site. Density-functional theory calculations show that the most stable strong bonding configuration involves the molecule sitting inside a seven-atom pit with 2.56 eV adsorption energy.

DOI: 10.1103/PhysRevB.82.125414 PACS number(s): 68.47.De, 68.37.Ef, 68.43.Fg, 71.15.Mb

INTRODUCTION

Surfaces with a regular array of energetic sites are useful templates for growing nanoscale structures from site-specific nucleation. A classical example of such a template is the (111) surface of gold which has been extensively studied as a standard system for the growth of ordered two-dimensional arrays of metal islands.[1–5] The so-called herringbone reconstruction[6,7] of Au(111) gives rise to a surface dislocation network which is able to direct the incoming atoms toward the well-defined reactive "elbow sites"[1,8] where nucleation of metal islands takes place. For organic molecules, preferential decoration of the elbow sites has also been observed but mostly at low temperatures.[9,10] In the case of C_{60} adsorption on Au(111) at room temperature (RT), the formation of closed-packed molecular monolayers has long been identified as a consequence of nucleation at step edges without any preferential attachment of C_{60} molecules to the elbow sites.[11–14] Recent investigations have revealed an interesting phenomenon about C_{60} adsorption on noble-metal surfaces such as Ag(111) and Cu(111). It has been reported that the bonding of C_{60} molecules on Ag(111) involves a single-atom vacancy.[15] An even dramatic seven-atom vacancy pit has been proposed for the adsorption of C_{60} on Cu(111).[16] The seven-atom vacancy pit on Cu(111) induced by C_{60} adsorption[16] is particularly interesting since a C_{60} molecule inside such a pit is effectively bonded to single-atom high steps in all directions. Such a bonding configuration is consistent with the preferential attachment of C_{60} molecules to step edges as well as the observed significant enhancement of the bonding strength between the first molecular layer and the metal substrate. On gold surfaces, nanopit formation following the adsorption of C_{60} molecules on Au(110) (Ref. 17) has also been reported and more recently a similar phenomenon has been proposed for the Au(111) surface[18] based on a study of close-packed single layer C_{60} islands. There have been so far no reports on the bonding configuration for individually adsorbed C_{60} molecules on Au(111) at room temperature. We report here the observation with scanning tunnel microscopy (STM) of individually adsorbed C_{60} molecules on the elbow sites of Au(111) at room temperature. By comparing with the behavior of the same molecule adsorbed on Au(111) at low temperatures[19] and performing density-functional theory (DFT) calculations, we identified two distinct bonding configurations with marked difference in their bonding strength. DFT calculations show that the strong bonding configuration at room temperature can be explained by the introduction of a single-layer deep pit below the adsorbed C_{60} molecule.

EXPERIMENT

The gold sample was prepared by thermal evaporation of gold onto a highly oriented pyrolytic graphite substrate at 650 K. The sample was then transferred to an ultrahigh-vacuum system where it was treated with several cycles of Ar^+-ion bombardment and thermal annealing. The resulting surface shows predominantly (111) oriented gold with many atomically flat regions up to 1–2 μm in size. The flat terraces exhibit the typical herringbone pattern consisting of $22\times\sqrt{3}$ reconstructed domains. C_{60} molecules were deposited onto the gold surface from a homemade Knudsen cell with a deposition rate of ~0.05 monolayer (ML)/min. STM images were acquired using an Omicron variable temperature (VT)-STM.

RESULTS AND ANALYSIS

Following a 0.015 ML deposition of C_{60} molecules at 46 K, the molecules are found to attach exclusively to the elbow sites on the Au(111) surface, either as individual molecules or in the form of small molecular clusters, Fig. 1(a). Detailed analysis of nucleation and growth of C_{60} islands at 46 K can

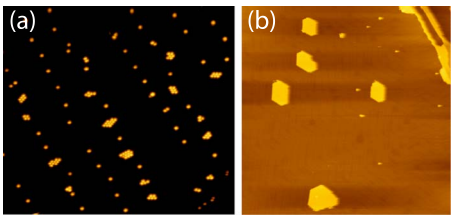

FIG. 1. (Color online) (a) Individual molecules and molecular clusters of C_{60} occupying the elbow sites at 46 K (74 nm $\times$82 nm, acquired with −3 V sample bias and 0.03 nA tunnel current). (b) STM image, 184 nm$\times$184 nm, showing step decoration (near the top right corner) and the formation of large molecular islands on the flat terrace upon thermal annealing to 284 K.

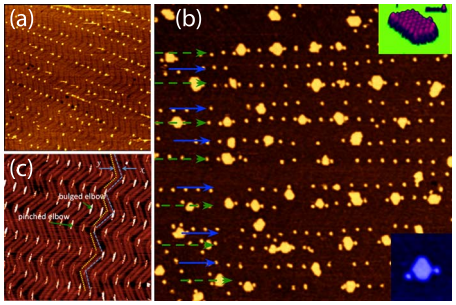

FIG. 2. (Color online) (a) STM image (200 nm×200 nm) showing the individually adsorbed C_{60} molecules at the elbow sites at room temperature. *Tunneling parameters for the image are* $V=-1.2$ V and $I=0.05$ nA. (b) The formation of the secondary structure in the form of molecular clusters. *Dashed* green arrows and solid blue arrows are used to draw attention to the two different types of islands. The inset at the upper right shows a 3D image of a typical small C_{60} island (α island) while the inset at the lower right corner shows a typical relationship between an α island and its two molecular "satellites." Tunneling parameters for the image are $V=-1.2$ V and $I=0.05$ nA. (c) STM image 100 nm×100 nm from the clean reconstructed Au(111) surface with $V=-0.02$ V and $I=12$ nA.

be found in Ref. 19. Subsequent heating of the sample causes the molecules to move out of the elbow sites. The first sign of molecules moving away from the elbow sites occurs at a temperature as low as 160 K. By 284 K, almost all the elbow sites are depleted of individually adsorbed molecules. Accompanying the disappearance of molecules from the elbow sites, we observed molecular aggregation along step edges and the nucleation and growth of some larger molecular islands on the Au(111) terraces as shown in Fig. 1(b).

The STM images in Fig. 1 show that while the elbow sites are capable of trapping individual C_{60} molecules at temperatures below 160 K, the local potential well at the elbow sites is not deep enough to retain the molecules at 284 K. Therefore, one would not normally expect to find individually adsorbed C_{60} molecules at the elbow sites if the molecules are deposited onto the sample at room temperature. It is thus surprising to us when we find individual molecules trapped at the elbow sites after room temperature deposition, Fig. 2(a). In this STM image one finds that, not only a few, but >70% of the elbows are occupied by individual C_{60} molecules. As more molecules are deposited onto the surface at RT, small molecular clusters (<6 nm in size) are found to form as shown in Fig. 2(b). A striking feature of the molecular clusters is that most of them are not nucleated from the preadsorbed individual molecules at the elbow sites. Rather, each cluster occupies the space between two isolated molecules and keeps a clear distance away from the isolated molecule on each side. This is in huge contrast to findings at 46 K where a molecular cluster always grows out of a single molecule preadsorbed at the elbow site.[19] The arrays of individually adsorbed molecules in Fig. 2(a) and molecular clusters in Fig. 2(b) are found on very large, atomically flat, terraces on the order of approximately micrometer. In regions where terraces sizes are less than ~100 nm, we find no individually adsorbed molecules and the compact islands are all attached to step edges.

The origin of surface aggregation of clusters on elbow sites or at step edges was analyzed previously where a curvature effect on physisorption was considered. A combined STM measurements and model calculations show that silver clusters on graphite, for instance, accumulate around concave regions.[20] Such an effect may also influence the C_{60} clustering process on Au(111). On a Au(111) surface, the discommensuration lines separating the fcc from the hcp region are known to belong to two types[1] as shown in Fig. 2(c). The *y*-type discommensuration lines bend rather gently at the elbows while the elbows along the *x*-type discommensuration lines are much more pointed. Along the *x*-type discommensuration lines, the elbows pointing to the direction of the fcc region are called bulge-out elbows and those pointing in the direction of the hcp region the pinch-in elbows. At the each elbow site, there is small group of "bright" atoms" when imaged with very small bias voltages indicating higher density of states near the Fermi level around these bright atoms. The *solid* blue arrows in Fig. 2(b) point to rows of bulge-out elbows.

A close examination of Fig. 2(b) reveals that there are two types of islands. One type, referred as the α island, is found to occupy the broad fcc region in between two pinch-in elbows. The α island is not in direct contact with the two individual C_{60} molecules already sitting at the pinch-in elbows, making the two C_{60} molecules at the opposite sides of each island look like two satellites as highlighted by the inset at the lower right corner of Fig. 2(b). The inset at the upper right corner shows a high-resolution three-dimensional (3D) image of an individual C_{60} island consisting of 35 molecules. In Fig. 2(b), rows of α islands, together with their "molecular satellites" are highlighted with green arrows. The solid blue arrows point to rows of the second type of island, β island, sitting on the narrow fcc region in between two bulge-out elbows. The β island is seen to swallow up the nearest C_{60} molecules at the bugle-out elbows and thus appears similar to the behavior of metal island nucleation on this surface.[3–5] The formation of the β islands on Au(111) is less favorable than that of the type-α islands. The majority of the C_{60} islands found in any region of the surface belong to type α. At 46 K, however, we found that molecular clusters are preferentially nucleated from the molecules preadsorbed at the bulge-out elbow sites, Fig. 1(a).

The behavior of C_{60} molecules adsorbed at RT and 46 K as shown in Figs. 1 and 2 is evidently very different. On one hand, results shown in Fig. 1 suggest that individually adsorbed molecules and small molecular clusters at 46 K are not stable beyond 284 K. On the other hand, data in Fig. 2 clearly show that individually adsorbed molecules at the elbow sites can be stable at RT (293 K). Moreover, the molecular clusters formed at RT have different characters from those formed at 46 K. This apparent "controversy" can only be resolved by considering two different bonding configurations for C_{60} molecules. It is known that gold atoms can jump out of the elbow site.[8] This, in conjunction with recent discoveries of C_{60} induced pit formation on Cu(111),[16] leads us to consider a bonding configuration where the C_{60} molecule sits either inside a big pit or above a small pit at RT.

We performed[21] DFT calculations to investigate adsorption energies of C_{60} molecules on one-, three-, and seven-

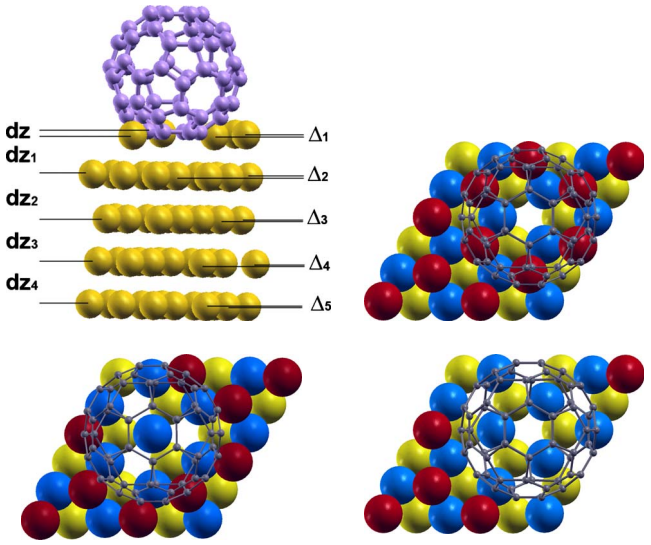

FIG. 3. (Color online) C_{60} molecules attached to vacancy sites on the Au(111) surface. (a) Side view of a C_{60} sitting on a seven-atom pit. (b)–(d) Top views of C_{60} on one-, three-, and seven-atom pits, respectively. First, second, and third layers of Au are shown in dark/red, gray/blue, and light/yellow, respectively.

atom pits. We used plane-wave expansion in conjunction with projector augmented wave[22] potentials, local-density approximations[23] as implemented in VASP.[24] Similar to that in Ref. 25, a seven-layer slab with two bottom layers fixed was employed to simulate the Au(111) surface, on top of which a monolayer C_{60} was adsorbed. The thickness of the vacuum between the molecule and neighbor metal surface was larger than 15 Å and a $(3\times3\times1)$ Monkhorst-Pack k-point mesh[26] was used.

For all the three vacancy-pit structures considered, the most stable configuration corresponds to a hexagon of the C_{60} in contact with the surface (shown in Fig. 3). The center of the hexagon aligns, in the z direction, with the center of the vacancy. Geometry optimization shows very little change in the C_{60} molecular structure in all three cases. We adopt the same procedure as in Ref. 15 to describe the surface reconstruction in the vertical (z) direction (see Table I). On average, atoms in the bottom hexagon of C_{60} molecules are 1.80 Å, 1.68 Å, and 0.15 Å above the first Au layer in one-atom, three-atom, and seven-atom pit, respectively. Comparing with a perfect Au(111) surface, the introduction of vacancies leads to a local contraction between the first layer and second layer Au atoms. We also calculated the intralayer buckling amplitude (Δ_i). For the one-atom and three-atom pits, there are relatively large amounts of buckling in the second layer, while for the seven-atom pit, the buckling amplitude is most significant in the first layer of gold.

To investigate surface reconstruction, we also examined the in-plane displacement of atoms near the three vacancies. Table I lists the calculated deviations of lateral positions [compared to positions in a perfect Au (111) surface] of those atoms right next the centers of vacancies. Only atoms in first and second layers show significant lateral displacement, denoted as Δ_{xy-1} and Δ_{xy-2}, respectively. Interestingly, atoms in the first layer appears to be repelled away from the center of

TABLE I. Structural parameters and adsorption energies: dz is the average interplane distance, Δ the average intralayer buckling amplitude, and Δ_{xy} the average lateral displacement of atoms surrounding a vacancy (see Fig. 3).

	One-atom pit	Three-atom pit	Seven-atom pit
dz (Å)	1.80	1.68	0.15
dz_1 (Å)	2.32	2.27	2.25
dz_2 (Å)	2.34	2.35	2.36
dz_3 (Å)	2.35	2.35	2.35
dz_4 (Å)	2.35	2.35	2.35
Δ_1 (Å)	0.04	0.05	0.10
Δ_2 (Å)	0.09	0.11	0.03
Δ_3 (Å)	0.01	0.01	0.03
Δ_4 (Å)	0.01	0.01	0.04
Δ_5 (Å)	0.01	0.01	0.01
Δ_{xy-1} (Å)	0.04	0.18	0.02
Δ_{xy-2} (Å)	−0.05	−0.06	0.03
Adsorption energy (eV)	2.07	2.33	2.56

vacancies, especially near the three-atom pit where atoms move by 0.18 Å; but in the second layer, atoms near a vacancy are attracted inward in the one-atom and three-atom cases. Small outward displacements of gold atoms are found for the first two layers in the vicinity of the seven-atom pit.

Calculated adsorption energies are 2.07 eV, 2.33 eV, and 2.56 eV for one-atom, three-atom, and seven-atom vacancies, respectively. Compared to a perfect Au surface of 1.2 eV,[24] the energy difference signals the cause of defect trapping of C_{60} since the translational motion of the molecule on a defect-free Au(111) is nearly barrier less. At 46 K, both individual molecules and small clusters appear 6.2 Å above the substrate surface in STM images. The individual molecules observed at room temperature measures ~4 Å, which is in good agreement with the seven-atom pit model shown in Figs. 3(a) and 3(d). Height measurement in STM is not always a reliable method for measuring geometric height of adsorbed species because of electronic effects. However, the 2.2 Å difference in measured heights is too large for a pure electronic effect. This height difference is in very good agreement with that measured for C_{60} molecules sitting on the upper terrace and those on the lower terrace sharing a common atom step.[27]

Pit formation is a thermally activated process, and our results show that at 46 K, seven-atom pit does not form on Au(111). Hence, molecules at the elbow sites at 46 K are in a weak bonding state. Increasing temperature promotes pit formation. However, the lifetime of diffusing molecules on surfaces decreases sharply with temperature. Trapping probability of individual C_{60} molecules by seven-atom pits is proportional to the concentration of pits and the concentration of diffusion molecules. The concentration of the elbow sites on Au(111) is not uniform because the discommensuration lines bend with different frequencies on different terraces. In the case where the surface consists of narrow terraces, the density of elbows is further reduced due to stress release via step edges. The other important factor is that step

edges are also effective trapping sites for diffusing molecules, thus they compete directly with molecular trapping by pits. Based on the above analysis, trapping of C_{60} by pits is more likely to occur on a large atomic terrace with a high density of elbows, and this is what we observed in our experiment. The gold sample prepared in our laboratory consists of atomic flat terraces extending to approximately micrometer, which is at least an order of magnitude larger than those found on typical single-crystal surfaces. For Au samples consisting only small terraces, C_{60} molecules should be expected to attach mostly to step edges at RT, as found in many previous studies.

Next, we discuss the nucleation of α and β islands. The STM image in Fig. 2(b) clearly shows that C_{60} islands prefer to occupy the fcc region of the surface. This is similar to that observed for some organic molecules[10] where it was shown that the dwell time of the molecules within the hcp domain is very short and hence nearly all molecules are found in the fcc domain shortly after landing on the surface. The same mechanism seems to apply to C_{60} molecules. Thus, we expect to see a higher number of C_{60} molecules diffusing along the length of the fcc region. The broad fcc region in between two pinch-in elbows can accommodate a relatively large number of molecules at any given time, thus nucleation of C_{60} islands in this region is favored. The reason that the individual C_{60} molecules already fixed at the pinch-in elbows do not become part of the island is because they are at the hcp region of the surface, and are separated from the fcc region by a *y*-type discommensuration ridge. The isolated C_{60} molecules at the pinch-in elbow sites thus do not directly participate in the formation of the α island. However, their presence on the surface may influence the energy-transfer efficiency between diffusion molecules and the gold substrate, making the region around the elbow as a local molecular trap.

The fcc region in between two bulge-out elbows is much narrower than that in between two pinch-in elbows. It is therefore less likely to accommodate a sufficient number of molecules there for nucleation to take place since stability of molecular clusters depends on their size. Once the nucleation of a β island does occur, the growth of such an island would engulf the preadsorbed single molecule which becomes part of the island. The reason for this is because at the bulge-out site, the bright atoms [see Fig. 2(c) where thin stripes of bright atoms appear at each elbow site] are located at the edge of the fcc region, so there is no discommensuration ridge separating the single molecule and the island. Compact C_{60} islands on Au(111) can have several orientations[11,13] relative to the crystallographic directions of the gold substrate. We find that the type-α islands are faceted and are confined in the fcc region by the domain walls. Their local structure is the same as the $2\sqrt{3}\times 2\sqrt{3}$ phase found for extended islands.[11,13] The β islands are found to have the in-phase orientation.[11,13]

CONCLUSION

In conclusion, we have discovered that the elbow sites on Au(111) can accommodate C_{60} molecules in two different bonding configurations. (i) Weak bonding at low temperatures: individual molecules occupy the elbow sites due to the existence of a high surface charge density at the elbows. The diffusion barrier is small for this bonding scheme. (ii) Strong bonding configuration at RT: molecules are trapped by seven-atom pits with adsorption energy 2.56 eV, which is significantly higher than the energy for a C_{60} sitting on a defect-free Au(111). The subsequent nucleation and growth of C_{60} clusters and compact islands are directly influenced by the initial bonding configuration of individually adsorbed molecules.

L.T., X.Z., and Q.G. thank the Engineering and Physical Sciences Research Council of the United Kingdom for financial support. H.-P.C. acknowledges the U.S. DOE under Grant No. DE-FG02-02ER45995 for supporting the work and U.S. DOE NERSC for computing resources.

[1] D. D. Chambliss, R. J. Wilson, and S. Chiang, J. Vac. Sci. Technol. B **9**, 933 (1991).
[2] A. W. Stephenson, C. J. Baddeley, M. S. Tikhov, and R. M. Lambert, Surf. Sci. **398**, 172 (1998).
[3] K. Morgenstern, J. Kibsgaard, J. V. Lauritsen, E. Lagsgaard, and F. Besenbacher, Surf. Sci. **601**, 1967 (2007).
[4] J. Biener, E. Farfan-Arribas, M. Biener, C. M. Friend, and R. J. Madix, J. Chem. Phys. **123**, 094705 (2005).
[5] Y. Zhang, N. Zhu, and T. Komeda, J. Phys. Chem. **111**, 16946 (2007).
[6] J. V. Barth, H. Brune, G. Ertl, and R. J. Behm, Phys. Rev. B **42**, 9307 (1990).
[7] Ch. Wöll, S. Chiang, R. J. Wilson, and P. H. Lippel, Phys. Rev. B **39**, 7988 (1989).
[8] H. Bulou and J. P. Bucher, Phys. Rev. Lett. **96**, 076102 (2006).
[9] T. Yokoyama, S. Yokoyama, T. Kamikado, Y. Okuno, and S. Mashiko, Nature (London) **413**, 619 (2001).
[10] M. Böhringer, K. Morgenstern, W.-D. Schneider, R. Berndt, F. Mauri, A. De Vita, and R. Car, Phys. Rev. Lett. **83**, 324 (1999).
[11] E. I. Altman and R. J. Colton, Surf. Sci. **279**, 49 (1992).
[12] C. Rogero, J. I. Pascual, J. Gomez-Herrero, and A. M. Baro, J. Chem. Phys. **116**, 832 (2002).
[13] X. Zhang, R. E. Palmer, and Q. Guo, Surf. Sci. **602**, 885 (2008).
[14] L. Tang, X. Zhang, and Q. Guo, Langmuir **26**, 4860 (2010).
[15] H. I. Li, K. Pussi, K. J. Hanna, L.-L. Wang, D. D. Johnson, H.-P. Cheng, H. Shin, S. Curtarolo, W. Moritz, J. A. Smerdon, R. McGrath, and R. D. Diehl, Phys. Rev. Lett. **103**, 056101 (2009).
[16] W. W. Pai, H. T. Jeng, C.-M. Cheng, C.-H. Lin, X. Xiao, A. Zhao, X. Zhang, G. Xu, X. Q. Shi, M. A. Van Hove, C.-S. Hsue, and K.-D. Tsuei, Phys. Rev. Lett. **104**, 036103 (2010).
[17] M. Hinterstein, X. Torrelles, R. Felici, J. Rius, M. Huang, S. Fabris, H. Fuess, and M. Pedio, Phys. Rev. B **77**, 153412 (2008).
[18] J. A. Gardener, G. A. D. Briggs, and M. R. Castell, Phys. Rev. B **80**, 235434 (2009).
[19] X. Zhang, L. Tang, and Q. Guo, J. Phys. Chem. C **114**, 6433 (2010).
[20] A. F. Kemper, H.-P. Cheng, N. Kébaïli, S. Benrezzak, M.

Schmidt, A. Masson, and C. Bréchignac, Phys. Rev. B **79**, 193403 (2009).
[21] W. Kohn and L. J. Sham, Phys. Rev. **140**, A1133 (1965).
[22] P. E. Blöchl, Phys. Rev. B **50**, 17953 (1994); G. Kresse and D. Joubert, *ibid.* **59**, 1758 (1999).
[23] D. M. Ceperley and B. J. Alder, Phys. Rev. Lett. **45**, 566 (1980); J. P. Perdew and A. Zunger, Phys. Rev. B **23**, 5048 (1981).
[24] G. Kresse and J. Furthmuller, Phys. Rev. B **54**, 11169 (1996); G. Kresse and J. Furthmuller, Comput. Mater. Sci. **6**, 15 (1996); G. Kresse and J. Hafner, Phys. Rev. B **47**, 558 (1993).
[25] L.-L. Wang and H.-P. Cheng, Phys. Rev. B **69**, 165417 (2004).
[26] H. J. Monkhorst and J. D. Pack, Phys. Rev. B **13**, 5188 (1976).
[27] L. Tang, X. Zhang, and Q. Guo, Surf. Sci. **604**, 1310 (2010).